Fiber Orientation Distribution Function Estimation by Spherical Needlets

Jie Peng

Department of Statistics, University of California, Davis

February 2016

Diffusion MRI

- Diffusion MRI is a magnetic resonance imaging technology which measures *diffusion* of water molecules along a set of (predetermined) directions.
  - In vivo, non-invasive, no radiation.
- Diffusion MRI uses water diffusion as a proxy to probe the anatomy of biological tissues.
- Raw data from a D-MRI experiment:
  - Multiple grey scale images corresponding to multiple gradient directions plus a few images with no diffusion weighting.
  - Each image consists of intensities for pixels on a 3D grid (e.g., $\sim 256 \times 256 \times 59$ for a human brain).
  - Image resolution: $1 \sim 3mm$.

D-MRI Provides Information on Brain Connectivity

- Neuron axons with similar destinations form big bundles called *white matter fiber tracts*.
- When applied to human brains, diffusion MRI reveals detailed anatomy of white matter tracts such as their location, size, shape and how they are connected to each other.
  - Human connectome project `http://www.humanconnectomeproject.org`.
- Alzheimer's Disease Neuroimaging Initiative (ADNI): `http://adni.loni.usc.edu/`.

Tractographic Reconstruction of Neural Connections

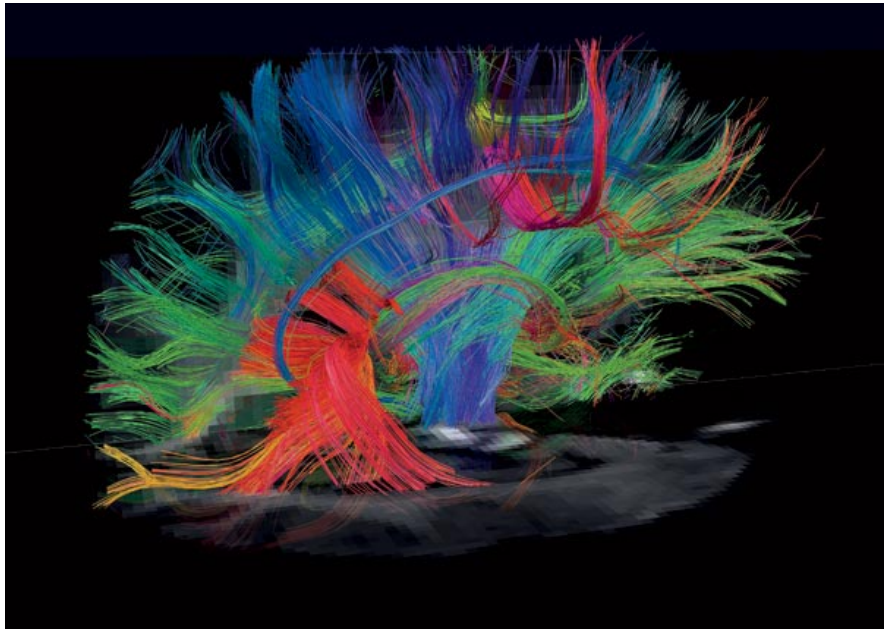

http://braintalks.wordpress.com/2011/12/04/10-maps-of-the-mind/

- With diffusion information at each voxel, fiber tracts can be reconstructed using computer-aided 3D tracking techniques called tractography.

Clinical Applications of Diffusion MRI

- Detect brain abnormality in white matter regions such as specific axonal loss, deformation in brain tumors.
- Differentiate types of tumor and growth orientation.
- Measure anatomy of immature brains.
- Monitor status of specific white matter tracts.

Water Diffusion in Biological Tissues

Anisotropic due to the presence of fibers with coherent orientations.

- Water tends to diffuse faster along fibers.
- Information on water diffusion may be used to probe tissue structure.

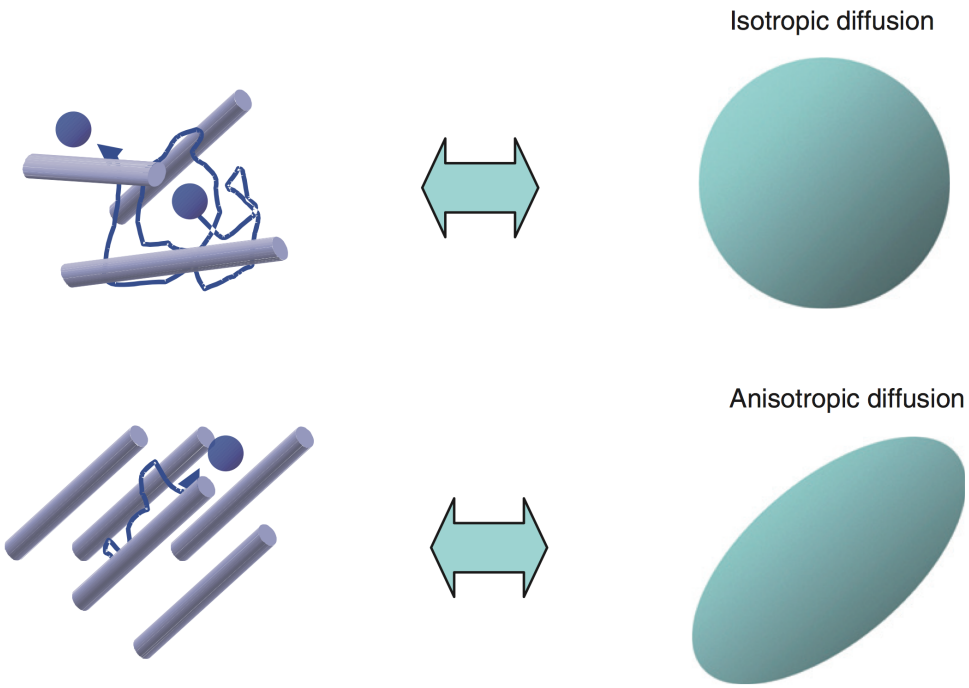

Diffusion in Brain

- White matter.
  - Astronomical number of connections: "cables" of the brain.
  - Presence of axonal bundles at image resolution ⇒ diffusion appears anisotropic.
- Grey matter.
  - ∼ 100 billion neurons: "CPU" of the brain.
  - Lack of coherent fiber organization at image resolution (∼2mm) ⇒ diffusion appears isotropic.

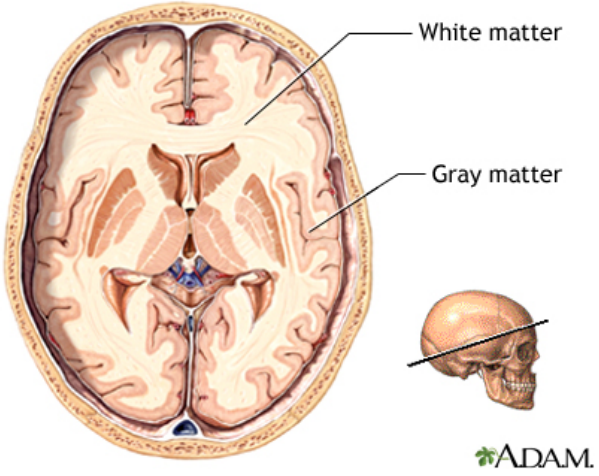

Sensitize MRI Signal by Water Diffusion

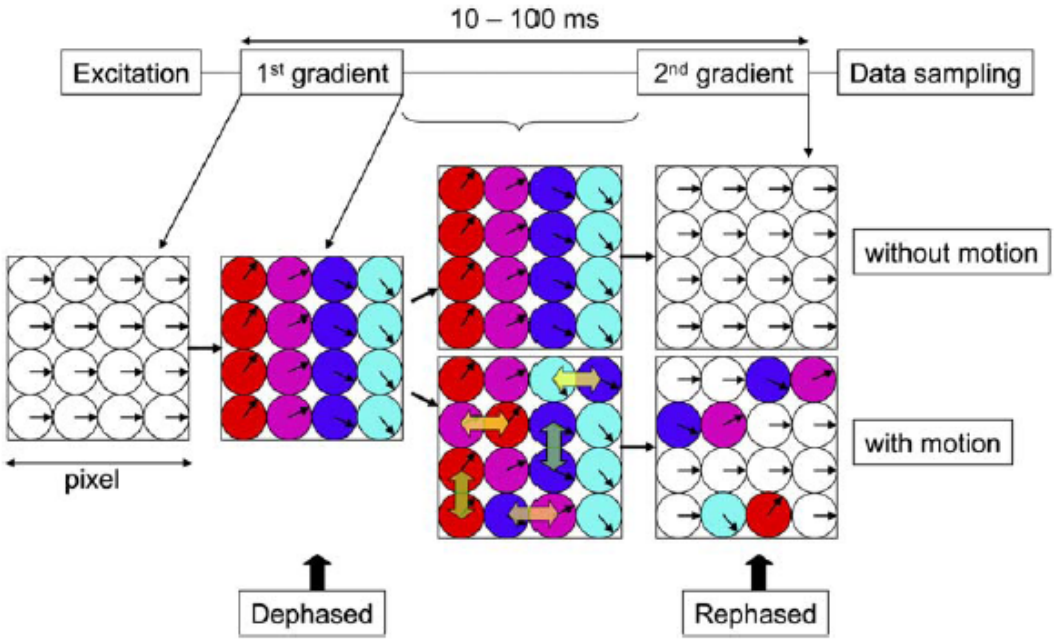

Mori and Zhang, 2006, Neuron 51

details

Diffusion Weighted Signals

At voxel $\mathbf{s}$, along direction $\mathbf{q}$, diffusion weighted signal:

$$S_0(\mathbf{s}) \int_{R^3} p_{\mathbf{s},\Delta t}(\mathbf{r}) \exp(i\gamma\delta\mathbf{q}\cdot\mathbf{r})d\mathbf{r}.$$

- $S_0(\mathbf{s})$: signal intensity without diffusion weighting at voxel $\mathbf{s}$.
- $p_{\mathbf{s},\Delta t}(\cdot)$: p.d.f. of water displacement in time duration Δt at voxel $\mathbf{s}$.
- Δt: time between "depahsing" and "rephasing".
- δ: duration of dephasing/rephasing.
- γ: gyromagnetic ratio.

Diffusion weighted signal is the inverse Fourier transform of the diffusion probability density function.

details

Gaussian Diffusion and Single Tensor Model

$$p_{\mathbf{s},\Delta t}(\mathbf{r}) = \frac{1}{(2\pi)^{3/2}} |\mathbf{D}(\mathbf{s})\Delta t|^{-\frac{1}{2}} \exp\left(-\frac{\mathbf{r}^\intercal \mathbf{D}(\mathbf{s})^{-1}\mathbf{r}}{2\Delta t}\right), \quad \mathbf{r} \in \mathbb{R}^3.$$

- $\mathbf{D}(\mathbf{s})$: **diffusion tensor**, a 3×3 p.d. matrix. Its principal eigenvector captures the fiber orientation within the voxel.
- DWI signal along gradient direction $\mathbf{u}$:

$$S(\mathbf{u}) = S_0 \exp(-b\mathbf{u}^T\mathbf{D}\mathbf{u}), \qquad b = \frac{\gamma^2\delta^2||\mathbf{q}||^2\Delta}{2}.$$

- $\mathbf{D}(\mathbf{s})$ can be recovered with as few as 6 distinct gradient directions.

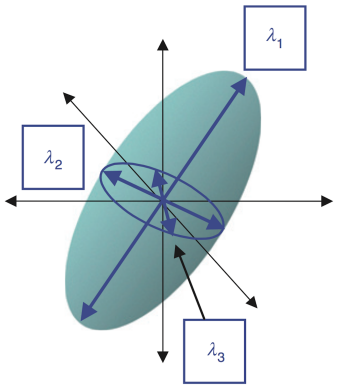

Crossing Fibers

More than 30% voxels have multiple fiber bundles with distinct orientations (under D-MRI image resolution).

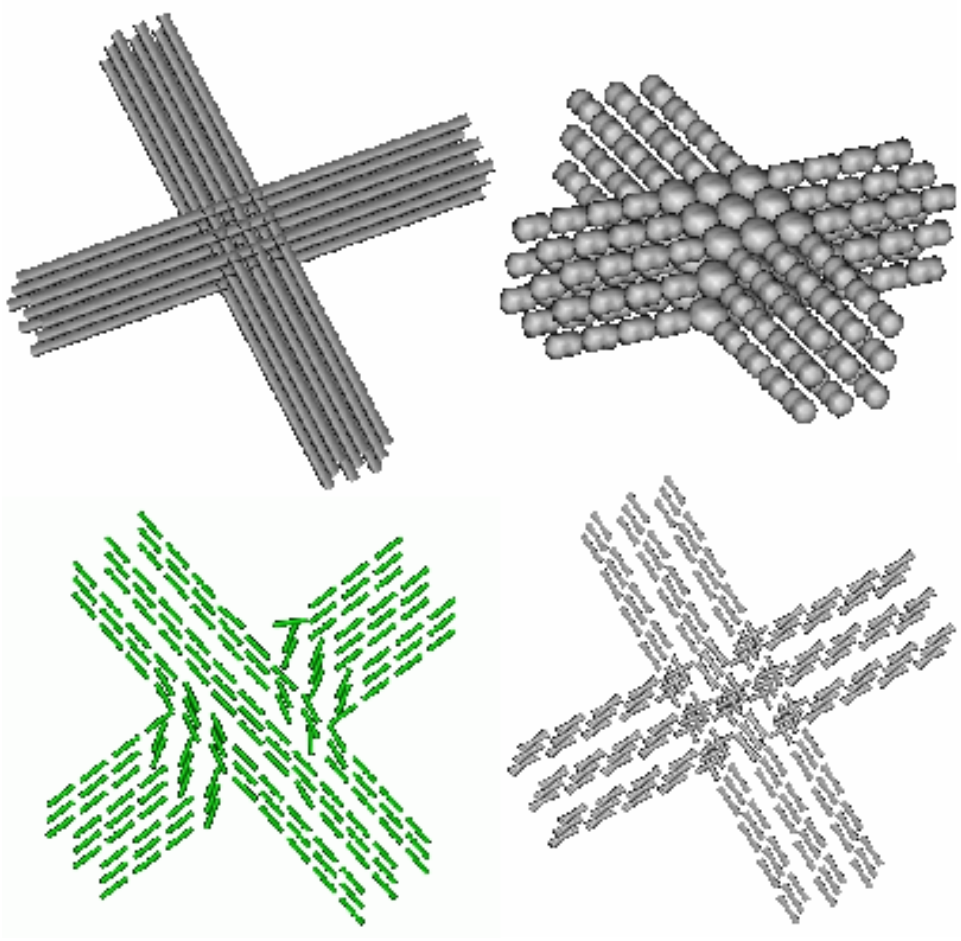

Limitations of Single Tensor Model

- Single tensor model can not resolve multiple fiber orientations within a voxel since a tensor only has one principal direction. It may incorrectly lead to:
  - Oblate ($\lambda_1 \approx \lambda_2 >> \lambda_3$) tensor estimation.
  - Low anisotropy and random diffusion directions.
  - Consequently, early termination of fiber tracking or bias/switching of fiber tracking.
- Tensor Mixture Model.
- **Nonparametric methods using HARDI data.**

HARDI Techniques

High angular resolution diffusion imaging (HARDI) techniques enable the detection of multi-modal diffusion signals.

- Q-ball imaging: Gradients are sampled from a single spherical shell of a particular radius (a single bvalue).
  - Diffusion orientation distribution function (ODF) (Tuch, 2004, Descoteaux et al., 2007).
  - Fiber orientation density (FOD) function (Tournier et al., 2004, 2007).

Fiber Orientation Density Function

FOD is a symmetric p.d.f. on $\mathbb{S}^2$ which describes the distribution of fiber orientations (corresponding to coherently oriented fiber bundles) at a voxel.

- Example. K distinct fiber bundles:

$$F(\theta, \phi) = \sum_{k=1}^{K} w_k \delta_{\theta_k, \phi_k}(\theta, \phi), \quad \theta \in [0, \pi], \quad \phi \in [0, 2\pi),$$

where $w_k > 0$, $\sum_{k=1}^{K} w_k = 1$ are the volume fractions and θ_k (polar angle) and ϕ_k (azimuthal angle) are the spherical coordinates of the k-th fiber direction.

Assumptions

- DWI signals are the summation of signals originated from distinct fiber bundles.
  - No water exchange between distinct fiber bundles.
  - No water exchange between orientationally distinct segments of the same fiber bundle.
- Diffusion characteristics along all fiber bundles are (i) identical no matter the direction or abundance of the fiber bundle, and (ii) *axially symmetric* around the fiber direction.
  - DWI signal from a single coherently oriented fiber bundle can be represented by an axially symmetric *response function*.
  - The response function is identical across fiber bundles.

Response Function

- An axially symmetric kernel

$$R : [-1, 1] \to \mathbb{R}$$

  which describes DWI signal resulting from water diffusion along a single fiber bundle aligned with the z-axis.
- Estimation of the response function. Assume response function is identical across voxels.
  - Fit the single tensor model to every voxel.
  - Identify voxels with high FA values and find their principal eigenvectors.
  - For each such voxel, rotate the DWI signals such that the principal eigenvectors are aligned with the z-axis.
  - Average the rotated DWI profiles across these voxels.

- Example. Gaussian diffusion with $\lambda_1 = \lambda_2 < \lambda_3$:

$$R(cos(\theta)) = S_0 \exp^{-b\mathbf{q}(\theta,\phi)^T \Lambda \mathbf{q}(\theta,\phi)} = S_0 \exp^{-b(\lambda_1 \sin^2\theta + \lambda_3 \cos^2\theta)},$$

where $\theta \in [0, \pi]$, $\mathbf{q}(\theta, \phi) = (\sin\theta\cos\phi, \sin\theta\sin\phi, \cos\theta)^T$ and $\Lambda = \mathrm{Diag}(\lambda_1, \lambda_2, \lambda_3)$.

- Since water diffuses fastest along the dominant fiber direction, the response function is attenuated the most along the z-axis.

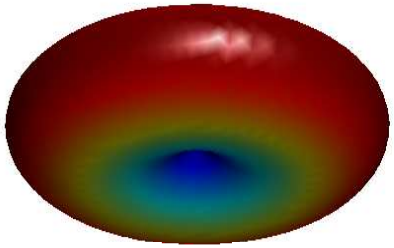

Figure: Gaussian diffusion response function with $\lambda_1 = \lambda_2 = 20, \lambda_3 = 1000$.

Spherical Convolution Model of Diffusion Signals

- DWI signal $S(\cdot)$ is the *spherical convolution* of the response function $R(\cdot)$ with the FOD $F(\cdot)$:

$$S(\mathbf{x}) = R \star F(\mathbf{x}) = \int_{\mathbb{S}^2} R(\mathbf{x}^T\mathbf{y})F(\mathbf{y})d\mathbf{y}, \quad \mathbf{x} \in \mathbb{S}^2.$$

- The FOD $F(\cdot)$ can be obtained by performing the *spherical deconvolution* of the response function $R(\cdot)$ from the DWI signal function $S(\cdot)$.
- Spherical deconvolution can be achieved through *spherical harmonic representation*.

Connection between the FOD model and the multi-tensor model.

- In the multi-tensor model, if the tensors D_k's have the same set of eigenvalues satisfying $\lambda_1 = \lambda_2 < \lambda_3$, then it corresponds to the FOD model with:
  - Response function

$$R(cos(\theta)) = S_0 \exp^{-b(\lambda_1 \sin^2\theta + \lambda_3 \cos^2\theta)}, \quad \theta \in [0, \pi],$$

  - FOD

$$F(\theta, \phi) = \sum_{k=1}^{K} w_k \delta_{\theta_k, \phi_k}(\theta, \phi), \quad \theta \in [0, \pi], \quad \phi \in [0, 2\pi),$$

where (θ_k, ϕ_k) denotes the principal eigenvector of the tensor D_k $(k = 1, \cdots, K)$.

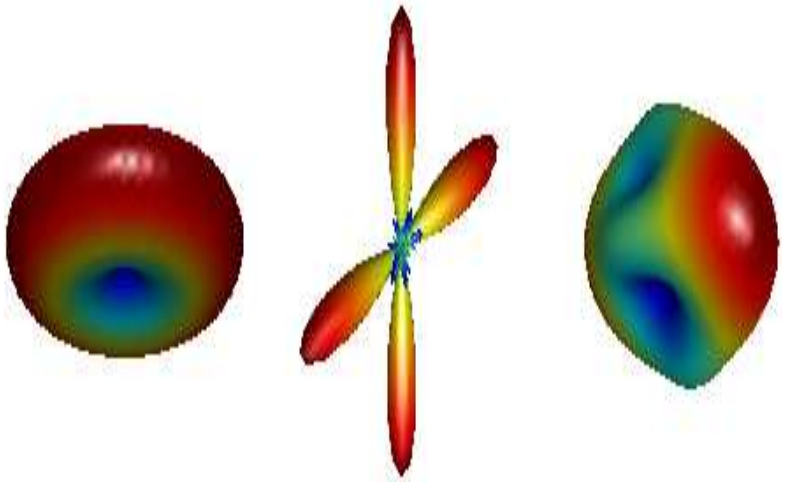

Figure: **Spherical Convolution**. Left to right: response function $R(\cdot)$, FOD $F(\cdot)$ and the DWI signal $S(\cdot)$.

Spherical Harmonics

- Spherical harmonics, denoted by $\tilde{\Phi}_{l,m}$:

$$\tilde{\Phi}_{l,m}(\theta,\phi) = \sqrt{\frac{2l+1}{4\pi}\frac{(l-m)!}{(l+m)!}}P_l^m(\cos(\theta))\exp^{im\phi},\ \ \theta \in [0,\pi], \phi \in [0,2\pi).$$

  - $l(\geq 0)$ denotes the harmonic order and m $(-l \leq m \leq l)$ denotes the phase factor.
  - Angular frequency increases with order l. Harmonics with even l are symmetric and those with odd l are anti-symmetric.
  - P_l^m is an associated Legendre polynomial of order (l, m).

Real Symmetric Harmonic Basis

- For $l = 0, 2, \ldots, l_{max}$ and $m = -l, \ldots, 0, \ldots, l$

$$\Phi_{l,m} = \begin{cases} \frac{\sqrt{2}}{2}(\tilde{\Phi}_{l,m} + (-1)^m \tilde{\Phi}_{l,-m}) & \text{if } 0 < m \leq l \\ \Phi_l^0 & \text{if } m = 0 \\ \frac{\sqrt{2}}{2i}((-1)^{m+1}\tilde{\Phi}_{l,m} + \tilde{\Phi}_{l,-m}) & \text{if } -l \leq m < 0 \end{cases}$$

- $\Phi_{l,m}$ form an orthnormal basis for real symmetric square-integrable functions (including R and F) defined on $\mathbb{S}^2$.

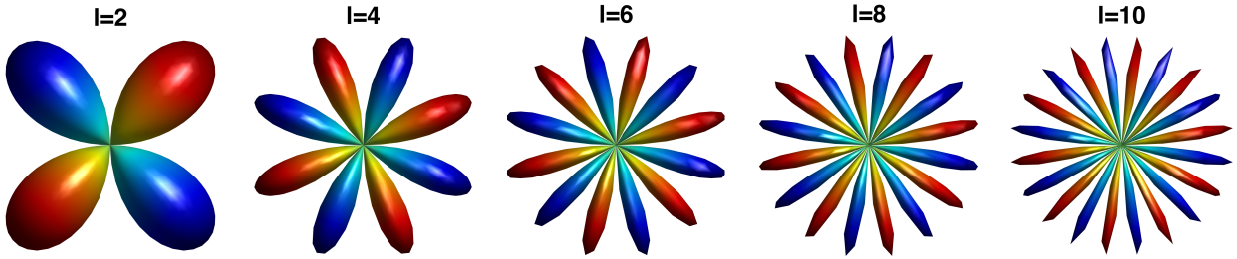

Figure: Real symmetric spherical harmonics.

- Since $S = R \star F$, so

$$s_{lm} = \sqrt{\frac{4\pi}{2l+1}} r_l f_{lm}, \quad l = 0, 2, 4, \cdots, m = -l, \cdots, 0, \cdots l,$$

  where $s_{lm} = \langle S, \Phi_{l,m} \rangle$, $r_l = \langle R, \Phi_{l,0} \rangle$ and $f_{lm} = \langle F, \Phi_{l,m} \rangle$ are the spherical harmonics (rotational harmonics) coefficients of S, R and F, respectively.
- Assume that $S(\cdot), R(\cdot), F(\cdot)$ can be represented by finite-order spherical harmonics functions $\{\Phi_{l,m} : -l \leq m \leq l\}_{l=0,2,\cdots,l_{\max}}$.
- The number of SH functions: $L = (l_{max} + 1)(l_{max} + 2)/2$.

Regression Model For DWI Measurements

The observed D-MRI signals:

$$\mathbf{y} = \mathbf{\Phi R f} + \boldsymbol{\epsilon}.$$

- $\mathbf{y} = (y(\theta_1, \phi_1), \cdots, y(\theta_n, \phi_n))^T$ is the $n \times 1$ vector of observed DWI measurements.
- $\mathbf{\Phi}$ is the $n \times L$ matrix of the SH functions evaluations at the n gradient directions $\{(\theta_i, \phi_i)\}_{i=1}^n$.
- $\mathbf{R}$ is an $L \times L$ diagonal matrix with diagonal elements $\sqrt{4\pi/(2l+1)}r_l$ (SH coefficients of the response function) in blocks of size $2l+1$ for $l = 0, 2, \cdots, l_{\text{max}}$.
- $\mathbf{f}$ is the $L \times 1$ vector of SH coefficients of the FOD F.

SH-ridge Estimator of FOD

- Penalized regression:

$$\widehat{\mathbf{f}} = \arg\min_{\mathbf{f}} \| \mathbf{y} - \mathbf{\Phi R f} \|_2^2 + \lambda \mathbb{E}(F), \quad F = \sum_{l,m} f_{l,m} \Phi_{l,m}$$

- Laplace-Beltrami penalty, $\mathbb{E}(F)$, a measure of roughness.

$$\mathbb{E}(F) := \int_{\Omega} (\Delta_b F)^2 d\Omega = \mathbf{f}^T \mathbf{P} \mathbf{f},$$

where $\mathbf{P}$ is a diagonal matrix with entries $l^2(l+1)^2$ in blocks of size $2l+1$.

- SH-ridge estimator:

$$\hat{\mathbf{f}}^{LB} = (\mathbf{R}^T \mathbf{\Phi}^T \mathbf{\Phi R} + \lambda \mathbf{P})^{-1} \mathbf{R}^T \mathbf{\Phi}^T \mathbf{y}, \quad \hat{F}^{LB} = \sum_{l,m} \hat{f}_{l,m}^{LB} \Phi_{l,m}.$$

Tournier et al.(2004).

sCSD Sharpening

Suppress small values of the estimated FOD and sharpens the peak(s) of the FOD estimator.

1. Initial step: Get an initial estimator $\widehat{\mathbf{f}}_0$ by SH-ridge.
2. At the $k+1$ updating step

$$\widehat{\mathbf{f}}_{k+1} = \arg\min_{\mathbf{f}} \| \mathbf{y} - \mathbf{\Phi R f} \|^2 + \lambda \| \mathbf{P}_k \mathbf{f} \|^2 \tag{1}$$

where $\mathbf{P}_k$ is an $n \times L$ matrix,

$$\mathbf{P}_{k,i,(l,m)} := \begin{cases} \mathbf{\Phi}_{i,(l,m)} & \text{if } \hat{F}_{k,i} < \tau \\ 0 & \text{if } \hat{F}_{k,i} > \tau \end{cases} \tag{2}$$

where $\hat{F}_{k,i}$ is the i the element of the vector $\hat{\mathbf{F}}_k = \mathbf{\Phi}\hat{\mathbf{f}}_k$

Tournier et al.(2007).

Spherical Needlets

- Spherical needlets $\psi_{j,k}$s are constructed from spherical harmonics functions (Nrcowich et al., 2006).
- Needlets are spatially localized with exponential concentration with respect to the frequency index j.
- Needlets provide sparse representations for spherical functions with small spatial scale features.

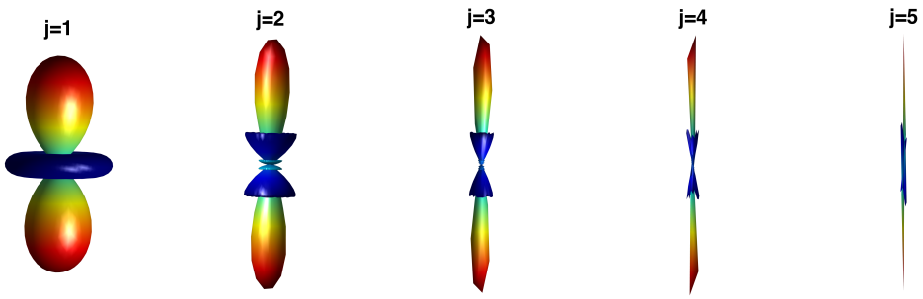

Figure: Real symmetric spherical needlets.

Needlets-lasso Estimator of FOD

- Assume that $S(\cdot), R(\cdot), F(\cdot)$ can be represented by finite-order spherical harmonics functions.
- Then they can be represented by finite needlets functions $\{\psi_{k,j} : k \in \chi_j\})_{j=0,\cdots,j_{\max}}$.
- The number of symmetric needlets: $N = 2^{2jmax+1} - 1$.
- There is a transition matrix $\mathbb{C}$ such that the spherical harmonics coefficients

$$\mathbf{f} = \mathbb{C}\boldsymbol{\beta},$$

  where $\boldsymbol{\beta}$ is the corresponding spherical needlets coefficients which are expected to be sparse.
- The observed D-MRI signals:

$$\mathbf{y} = \boldsymbol{\Phi}\mathbf{R}\mathbb{C}\boldsymbol{\beta} + \boldsymbol{\epsilon}.$$

ℓ_1 penalized regression with nonnegativity constraints:

$$\hat{\boldsymbol{\beta}} = \arg \min_{\boldsymbol{\beta}:\tilde{\boldsymbol{\Phi}}\mathbb{C}\boldsymbol{\beta}\geq 0} \| \mathbf{y} - \boldsymbol{\Phi}\mathbf{R}\mathbb{C}\boldsymbol{\beta} \|_2^2 + \lambda \| \boldsymbol{\beta} \|_1 .$$

- λ is a tuning parameter which controls the degree of sparsity.
- $\hat{F}^{NL} = \tilde{\boldsymbol{\Phi}}\mathbb{C}\boldsymbol{\beta} \geq 0$ ensures that the estimated FOD is nonnegative on the evaluation grid.
- This is a constrained convex minimization problem and can be solved by the ADMM algorithm.

Simulation Setting

- FODs with two distinct fiber bundles:

$$F(\theta, \phi) = w_1 \delta(\theta_1, \phi_1) + w_2 \delta(\theta_2, \phi_2).$$

- $w_1 = w_2 = 0.5$.
- Separation angle between the two fiber bundles: $\theta_{sep} = 45, 60, 75, 90$ degrees.
- Gaussian diffusion response function with $\frac{\lambda_3}{\lambda_1} = 50$.
- $n = 81$ gradient directions, sampled from an equal angle grid.
- bvalue=$1000 s/mm^2$, $3000 s/mm^2$.
- $SNR = \frac{S_0}{\sigma} = 20$, where S_0 is the b_0 image intensity and σ is the Rician noise standard deviation.

The number of gradient directions, SNR and bvalue are typical/close to those in real D-MRI studies.

Simulation Results

- FODs are estimated by SH-ridge with $l_{\max} = 8$ ($L = 45$ SH functions), by sCSD sharpening, and by needlets-lasso with $j_{\max} = 4$ ($N = 511$ needlets functions).
- Tuning parameters in SH-ridge and needlets-lasso are chosen by BIC. Those of sCSD are set as the recommended values by the paper.
- The needlets-lasso estimator has much sharper peaks.
- sCSD is sensitive to the penalty parameter τ as well as $l_{\max}$ and thus is hard to automate in the real data setting where there are hundreds of thousands voxels with different fiber population characteristics.

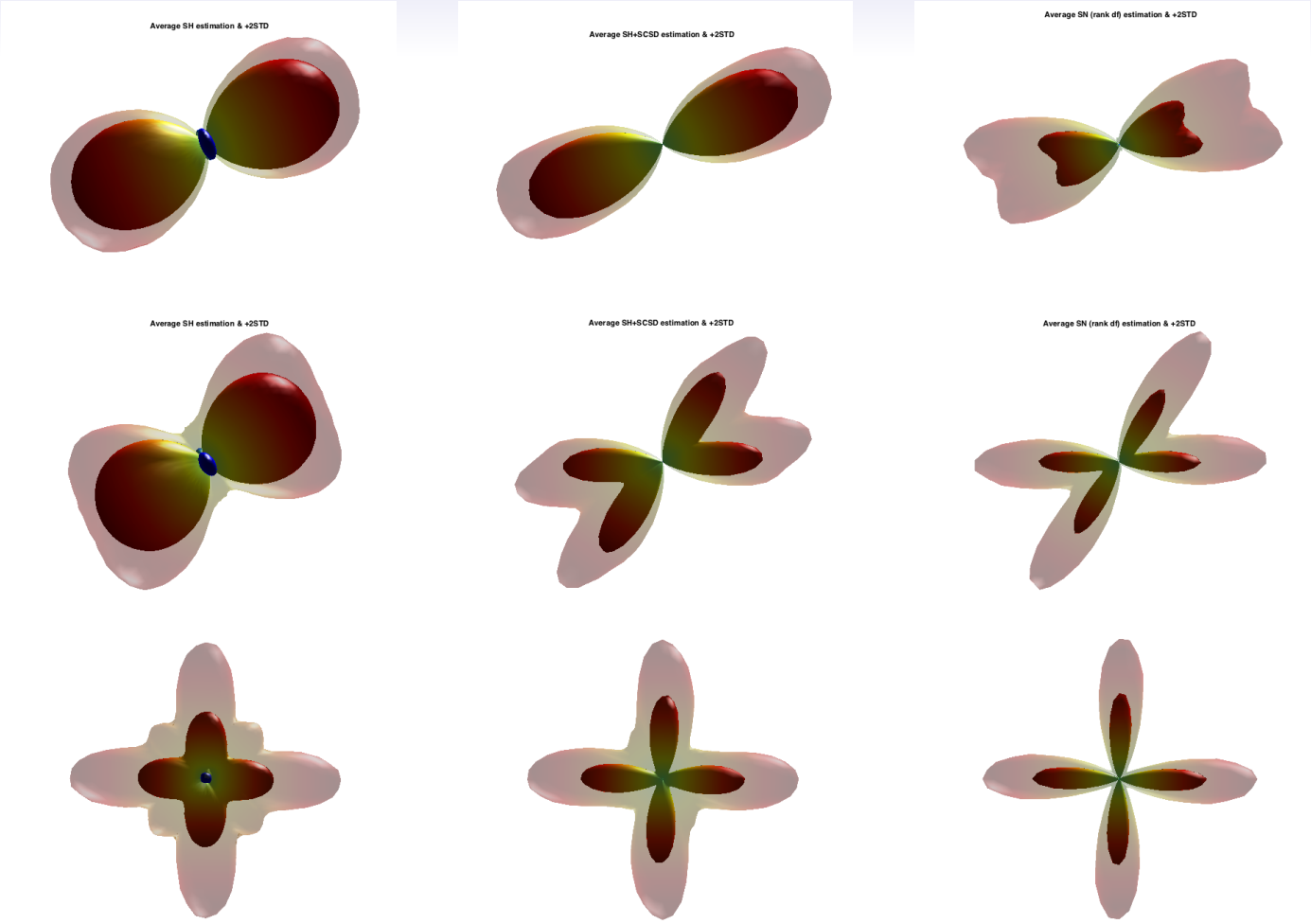

Figure: Mean plus 2-SD plots across 100 replicates. bvalue=1000. Top: $\theta_{sep} = 45$; Middle: $\theta_{sep} = 60$; Bottom: $\theta_{sep} = 90$. Left: SH-ridge; Middle: sCSD; Right: needlets-lasso.

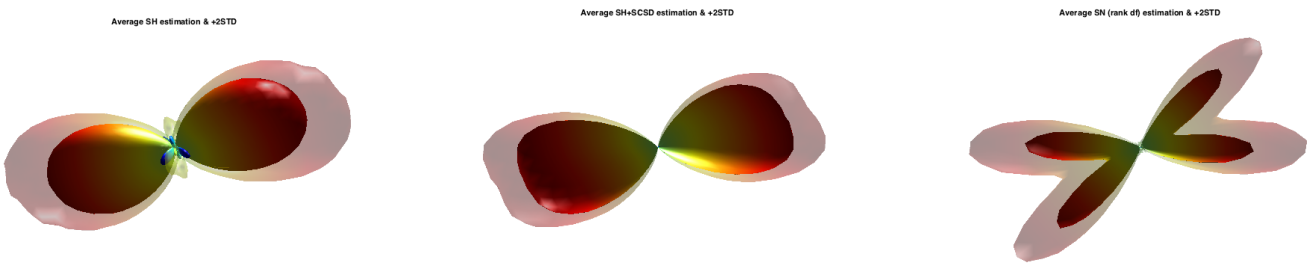

Figure: Mean plus 2-SD plots across 100 replicates. bvalue=3000. $\theta_{sep} = 45$. Left: SH-ridge; Middle: sCSD; Right: needlets-lasso.

Three fiber bundles simulation.

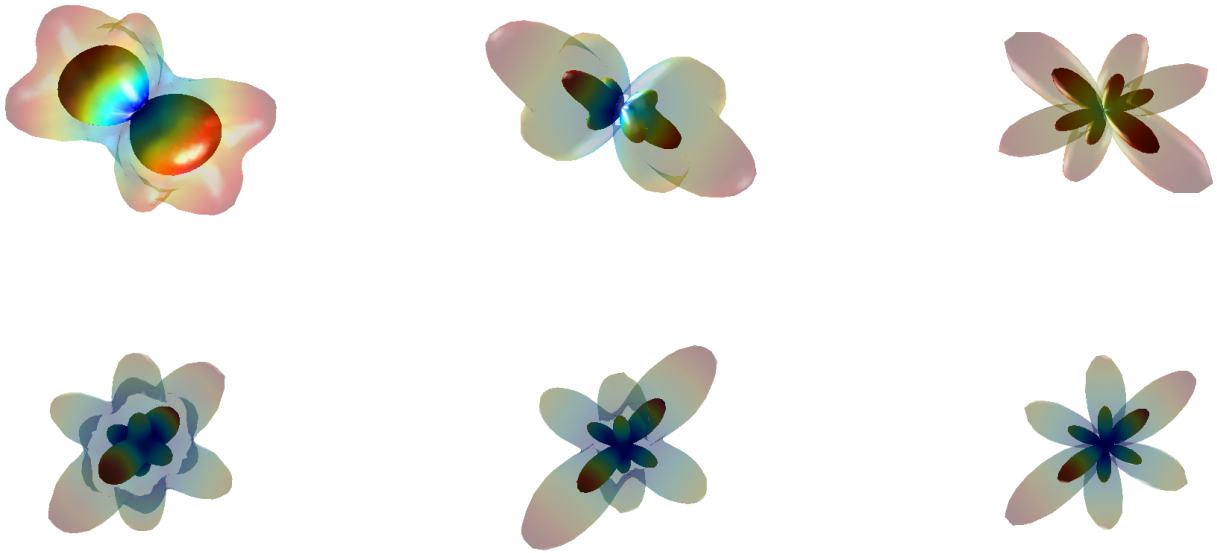

Figure: Mean plus 2-SD plots across 100 replicates. bvalue=1000. Top: $\theta_{sep} = 75$; Bottom: $\theta_{sep} = 90$. Left: SH-ridge; Middle: sCSD; Right: needlets-lasso.

Discussion

- Borrow information from neighboring voxels.
- Inference based on bootstrapping.
- Feature extraction and multiscale analysis.

Sensitize MRI Signal by Water Diffusion

- *Excitation*: Apply a strong homogeneous field $\Rightarrow$ water molecules resonate at the same frequency and phase.
- *Dephasing* : Apply a linearly inhomogeneous gradient field $\Rightarrow$ water molecules resonate at different frequencies depending on their locations.
- Apply the homogeneous field $\Rightarrow$ water molecules resonate at the same frequency again, but signal is still out of phase.
- *Rephasing*: Apply an opposite gradient field.
  - If water molecules had moved along the gradient direction, then there would be a disruption of phase $\Rightarrow$ signal loss and signals are *diffusion weighted*.

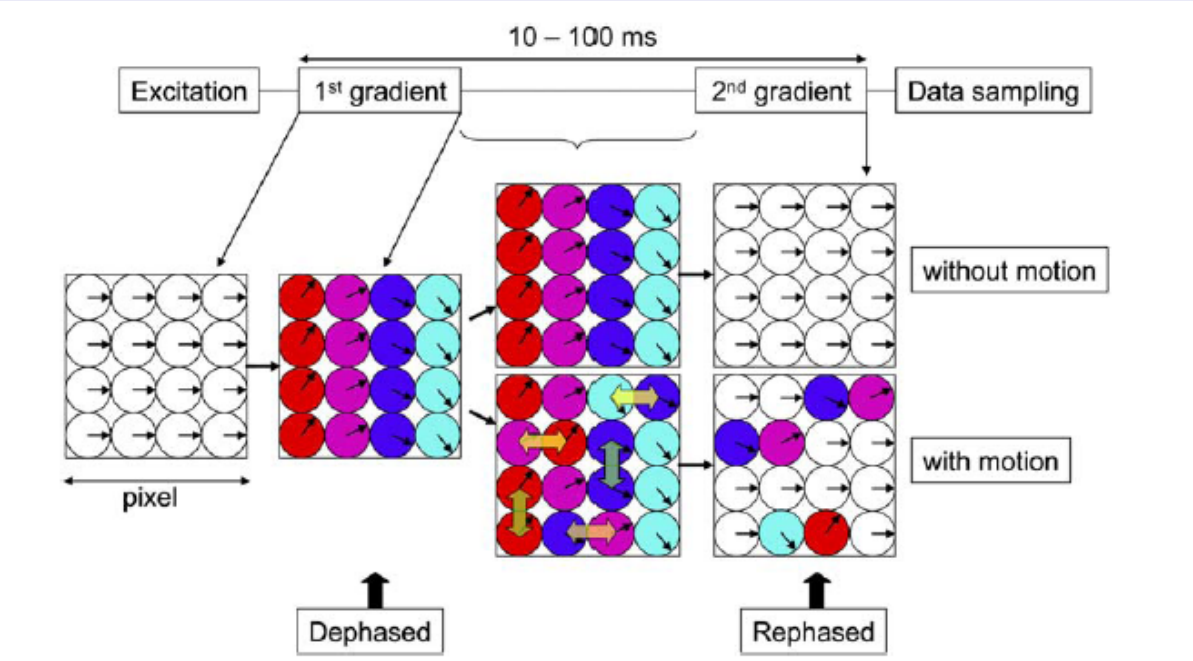

Mori and Zhang, 2006, Neuron 51

MRI can not measure the phase of individual water molecules, but it can detect imperfect rephasing through signal loss.

- During MR measurements, the amount of water molecular displacement is about $1 \sim 20\mu m$, depending on sample, temperature, duration of experiment, etc.
- DT-MRI experiments are designed such that this amount of diffusion leads to $10 \sim 90\%$ signal loss.

Diffusion Weighted Signals

- "Dephasing" encodes the location information of water molecules through their signal phase.
- MR can not measure the phase of individual water molecules, but it can detect imperfect rephasing through signal loss.
  - Perfect rephasing only happens when water molecules remain stationary between the two applications of gradients.
  - If water moved between "dephasing" and "rephasing", there will be a disruption of phase across the sample.
  - Then after rephasing, some of the molecules that moved will have different phases from the stationary molecules. This leads to an overall signal attenuation – signals are *diffusion weighted*.
- Water motion along directions perpendicular to the gradient direction will not cause signal loss and thus can not be detected.
  - Multiple gradient directions need to be applied if water diffuse anisotropically.

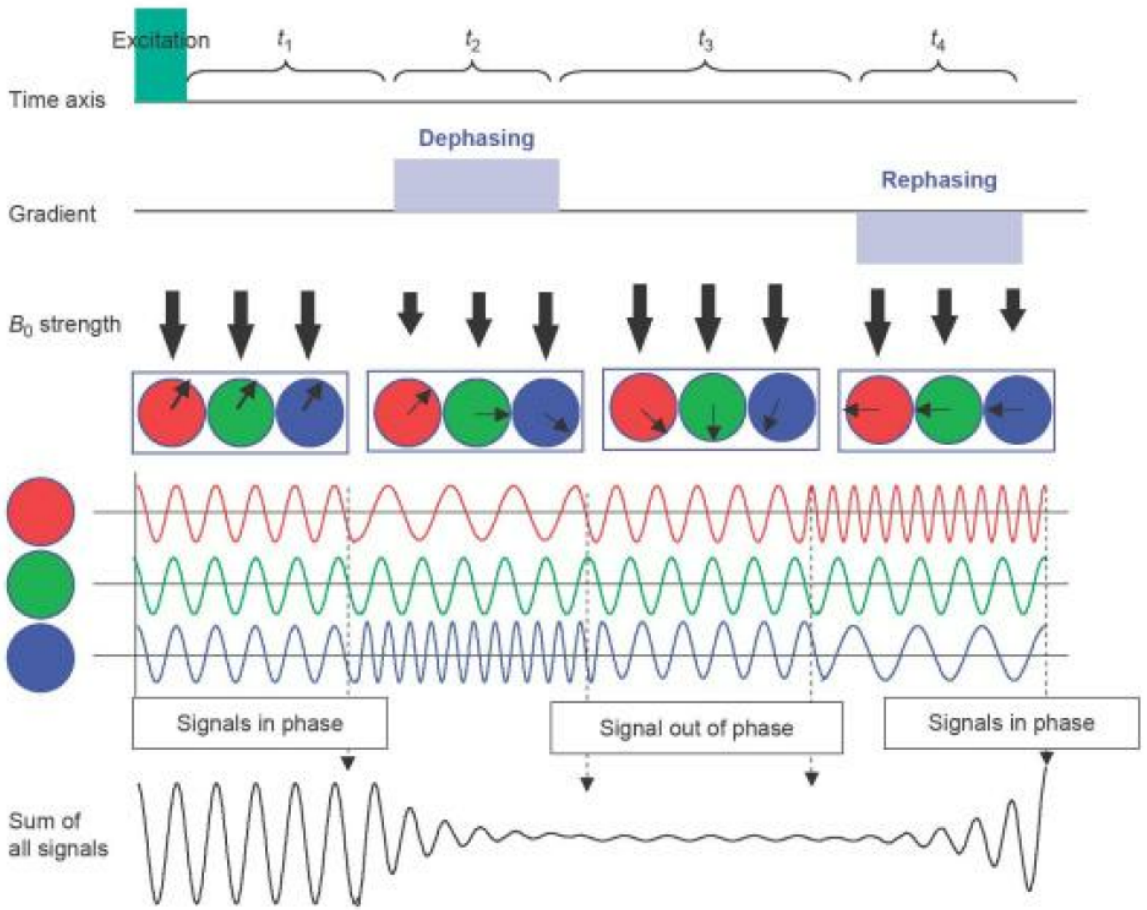

Fig. 1.9 An example of a dephase–rephase experiment by gradient application. Red, green, and blue circles indicate three water molecules located at different positions in a sample tube. Thick arrows indicate the strengths of magnetic field strength (B_0), and narrow arrows indicate phases of MR signals from each molecule.

Introduction to diffusion tensor imaging, Mori, 2007

back

Model Diffusion Signals

- Signal loss equals to the summation (across locations within a voxel) of the sinusoid waves with shifted signal phases weighted by the proton density at their corresponding location.
- Applying a gradient field $\mathbf{q}$ with duration δ introduces a *phase shift* in space:

$$\gamma\delta\mathbf{q}\cdot\mathbf{r}, \quad \mathbf{r}\in R^3$$

  which is proportional to the projected distance on $\mathbf{q}$.
  - $\mathbf{q}\in R^3$ – gradient field: $||\mathbf{q}||$ – field strength, $\mathbf{u}=\mathbf{q}/||\mathbf{q}||$ – gradient direction.
  - $\mathbf{r}\in R^3$: displacement vector.
  - δ: duration of dephasing/rephasing (assumed to be short, so ignore water movement during δ).
  - γ: gyromagnetic ratio.

back

- After the "dephasing" stage, water molecules start to move during the time period Δt ($>> \delta$). Their final locations are distributed according to a *diffusion probability density function*:

$$p_{\Delta t}(\mathbf{r}), \quad \mathbf{r} \in R^3$$

– density of protons having a displacement $\mathbf{r}$ in time duration Δt.

  - Δt: time between "depahsing" and "rephasing". Typically, the molecular displacement is $1 \sim 20\mu m$.
  - The probability of water molecules having displacements $\mathbf{r}$ and $-\mathbf{r}$ is the same:

$$p_{\Delta}(\mathbf{r}) = p_{\Delta}(-\mathbf{r}).$$

back

Microscopic vs. Macroscopic

- The average distance that water molecules move during the MR measurement is $1 \sim 20\mu m$.
- Thus only barriers that have a smaller dimension may cause anisotropy in water diffusion, this includes microscopic cellular architecture ($< 10\mu m$) such as protein filaments, cell membrasnes, myelin sheaths.
- However, the image resolution is much coarser ($\sim 2mm$). Therefore information is averaged within each voxel.
- Thus **diffusion MRI provides information on "macroscopic coherent arrangement of anisotropic microscopic anatomy"** (Mori, 2007). Only when both factors exist in a voxel, one can observe diffusion anisotropy.

Spherical Needelts Construction

- Two main ideas: (i) discretization of the sphere by an exact quadrature formula; (ii) Littlewood-Paley decomposition.
- The quadrature formula discretizes the sphere into cubature points and cubature weights:

Theorem 1. *Denote $\mathcal{H}_l$ as the space spanned by $\{Y_{lm} : m = -l, \cdots, l\}$, and let $\mathcal{K}_l = \bigoplus_{k=0}^{l} \mathcal{H}_k$. For any $l \in \mathbb{N}$, there exist a finite subset $\mathcal{X}_l = \{\xi_{lk} : k = 1, \cdots, n_l\}$ of $\mathbb{S}^2$ and positive real numbers $\{\lambda_{lk} : k = 1, \cdots, n_l\}$ such that*

$$\int_{\mathbb{S}^2} f(\boldsymbol{x}) d\boldsymbol{x} = \sum_{k=1}^{n_l} \lambda_{lk} f(\xi_{lk}), \tag{7}$$

for any $f \in \mathcal{K}_l$. Here ξ_{lk} and λ_{lk} are called cubature points and cubature weights, respectively.

Spherical Needelts Construction (Cont'd)

- Given a frequency $j \in \mathbb{N}_0$ and cubature points ξ_{jk} and weights λ_{jk}, the spherical needlets with frequency j ($B > 1$):

$$\psi_{jk}(x) = \sqrt{\lambda_{jk}} \sum_{l=\lfloor B^{j-1} \rfloor}^{\lceil B^{j+1} \rceil} b\left(\frac{l}{B^j}\right) \sum_{m=-l}^{l} \tilde{\Phi}_{l,m}(\xi_{jk}) \overline{\tilde{\Phi}}_{l,m}(x), \quad x \in \mathbb{S}^2.$$

- $b(\cdot)$ is a window function satisfying: (i) $supp(b) = [1/B, B]$; (ii) $\sum_{j=0}^{\infty} b^2(t/B^j) = 1$, for any $t > 0$; (iii) $b \in C^{(M)}$ for some $M \geq 1$.
- $b(\cdot)$ decomposes the frequency domain into several overlapping intervals (B^{j-1}, B^{j+1}).
- ξ_{jk} determines the location of the needlets ψ_{jk} and λ_{jk} determines to what extent ψ_{jk} is localized.
- Varying ξ_{jk} and j is analogous to translation and dilation in multiscale analysis.

Spherical Needlets Properties

- Needlets are real-valued spherical functions.
- They are localized in the frequency domain since the window function has compact support.
- Needlets are spatially localized with exponential concentration with respect to the frequency index j.
- Spherical needlets provide sparse representation of spherical functions with sharp local peaks.
- Needlets (together with the first spherical harmonics $\tilde{\Phi}_{00}$) form a tight frame on $L^2(\mathbb{S}^2)$:

$$\|f\|_{L^2}^2 = \sum_{j,k} |\langle f, \psi_{jk}|^2 + a_{00}^2.$$

- They are almost orthogonal: for $|j - j'| \geq 2$, $< \psi_{jk}, \psi_{j'k'} >= 0$.
- The spherical needlets ψ_{jk} and $\psi_{jk'}$ are asymptotically uncorrelated as the frequency j increases and the distance between them remains fixed.

back